Contents

Chapter 2

Ab initio simulation of amorphous materials

Rajendra Thapa[1], David A. Drabold[1]

2.1 Introduction

2.1.1 Big picture

Experiments on materials determine our state of knowledge about the physical world. Such experiments come in all shapes and sizes. Diffraction of X-rays, neutrons or electrons convey essential information about local ordering of atoms, EXAFS gives specific information about local structural order derived from the electronic structure of the system. The electronic density of states can be indirectly measured by photoemission experiments or inferred from optical absorption. The electronic tail states are built from valence and conduction states near the Fermi level and are the key to doping, transport and optics. The vibrations of the network are essential to understanding thermal and mechanical properties.

These experiments never uniquely identify the structure of matter in an amorphous state (in the sense of providing atomic coordinates), and many such measurements require intricate computations to interpret their meaning. Experimentally validated computer models can convey reliable atomistic information about the material.

We argue then, that to understand disordered phases of condensed matter, a full set of experiments and realistic computer models are required. Naturally, obtaining convergence between experiments and theory is necessary and can sometimes be an iterative process. As a point of logic, the more experiments we have, the more information we possess about the material. The information intrinsic to a neutron diffraction experiment is very different than a measurement of optical absorption or vibrations. In principle as each new experiment is performed, we should create models anew to jointly satisfy *all* the experiments. And it is not uncommon to find that one experiment is relatively ”easy” to represent and others might be quite difficult. We show that usually highly accurate “*ab initio*” interatomic interactions are required for these complex

---

[1] Department of Physics and Astronomy, Nanoscale and Quantum Phenomena Institute, Ohio University, Athens, OH.

systems.

2.1.2 The limits of experiment

2.1.2.1 The scourge of averaging

Most measurements on materials involve macroscopic numbers of atoms, and thus are an average over myriad local environments, hence the smoothing (compared to crystals) of measured observables. Local probes of materials are important and are especially relevant to amorphous materials if the spatial resolution of the experiment is fine enough to detect variation in local environments. Perhaps the ultimate example of a local probe is atomic resolution scanning tunneling microscopy (STM). Techniques like micro Raman can probe materials on a *ca.*1 micron length scale. Obviously enough, all "spectroscopic" techniques face related challenges: to get a measurable spin-resonance, Raman, IR... signal, many atoms are needed to enable the measurement, and the signal is necessarily averaged over these. Electronic and transport measurements suffer analogously. So for disordered systems, experiments do not usually offer direct information about atomic scale disorder, but instead provide "sum rules" (structural, electronic, and otherwise) that a good computer model must satisfy.

2.1.2.2 Diffraction

For crystals it is usually possible to "invert" the structure from diffraction measurements. The intuitive reason is that the information contained in a palisade of Bragg peaks[1] is vast – mathematically speaking it is approximately a collection of Dirac δ functions with intensity and energy precisely defined. By contrast, the diffraction structure factor S(q) (or the pair-correlation function $g(r)$) is smooth and the information is commensurately reduced. For sufficiently large distances in space, $g(r)$ asymptotically approaches unity, implying no further structural information. Protein crystallography is one of the great triumphs of modern science, with more than 100,000 entries in the Protein Database and 20 Nobel Prizes[2]. Yet this glittering success depends entirely on the incredible possibility of crystallizing the proteins, and thus cannot help us with our non-crystalline systems.

Diffraction data provides only pair correlations, and it is also blind to chemical order: only the total structure factor is usually measured, so that in a material with (say) two atomic species, we get information about all pair distances with no chemical specificity. The method of isotopic substitution, successfully demonstrated by Salmon *et al.*[3], exploits the fact that neutron scattering lengths can depend strongly on the particular isotope present and thus enables the extraction of partial pair correlations. The method is an important advance, but is not always readily applied to arbitrary materials (since it depends on the availability of possibly rare isotopes to fabricate samples large enough to produce high quality diffraction data). Satisfying diffraction data is necessary but certainly *not* sufficient to guarantee that a computer model is realistic.

2.1.2.3 Spectroscopic information

A wide variety of spectroscopic experiments are available and provide valuable information about materials. Meaningful comparisons with models require accurate computations of the electronic, optical and possibly vibrational properties of the computer models. And of course spectroscopic methods are subject to the scourge of averaging!

2.1.3 Synergy between experiment and modeling

Disordered materials are a classic arena for the interplay between experiment, theory and simulation. While we have criticized the limitations of information carried by experiment, there are serious limitations in modeling too (systems so small that they are not obviously physically relevant or adequately sampling the local bonding environments – the opposite of the “averaging” charge lodged above against experiments), inaccuracies in atomic interactions, basic challenges to computing physical observables reliably (as for example accurately computing an optical spectrum), simulation times that are many orders of magnitude removed from all but the fastest spectroscopies. We face a difficult limit: we need accurate interactions, large systems and often extended (say nanosecond) simulation time or a thorough exploration of configuration space that will sample representative local structures. Every “computational knob” should be on maximum for these calculations.

Thus, the respective warts of the experiment and modeling paradigms are limited in opposite ways and if we can bridge the gap between them, then we can gain new and reliable insight into these materials and learn about the limitations of the methods themselves[4].

2.1.4 History of simulations and the need for ab initio methods

The first recognizable MD simulation was carried out by a Swedish astronomer, Erik Holmberg during the second World War [5]. He took advantage of the identical radial r^{-2} dependence of the light intensity with distance from a point source, and the gravitational force to enable simulations based upon an “optical analogy” of the gravitational interaction. Holmberg constructed a clever apparatus in which two groups of 37 lamps each (each lamp representing a star, each group representing a galaxy) interacted optically, and the light intensity at each lamp (“star”) was measured with selenium photocells. Since the light intensity was proportional to the interstellar forces, the time evolution of a galactic collision could then be simulated with a “mechanical Eulers’ method”, and Holmberg was able to see spiral arms and draw inferences about galactic scattering and capture probability.

Early simulations of liquids and materials used *ad hoc* potentials and moved atoms according to classical mechanics (Newton’s second law). The primitive computers (and smart scientists) of the time could directly simulate the dynamics of systems with hundreds or thousands of atoms or molecules[6]. While the potentials were crude by modern standards, an impressive amount was learned, and the experience gained with empirical potentials with integration methods, size artifacts, alternate ”ensembles” (meaning simulations with different fixed thermodynamic variables) and many other aspects of simulation transferred immediately to the *ab initio* simulations we emphasize here. A classic work in this area is the book of Allen and Tildesley[7].

The first MD simulations used empirical potentials: functions made up to mimic some known behavior about a material. Such a potential might be designed to reproduce the right ground state crystal structure, melting points etc. The trick for such calculations is applying the potential to a structure with different local bonding – as for example carrying out a simulation for an amorphous solid or say a small molecule for a potential that was designed to fit a crystal. Such simulations are hit or miss, and often fail qualitatively. A potential that works in all salient bonding environments is called “transferable”. Some potentials with directional covalent bonding have limited transferability in different bonding environment.

Why is it so difficult to make a generally reliable interatomic potential? The answer is short: *electrons*. Consider the ground state conformations for a series of small Si molecules: Si_2, Si_3, Si_4... Start with a pair of Si atoms. Pair interactions are obviously adequate, and the ground state separation between the atoms is at the minimum in the pair potential energy function $V_2(\mathbf{x_1}, \mathbf{x_2})$ for the dimer. Now add a third atom in the vicinity of the pair. To minimize the energy of the trimer, covalent bonds form between all three atoms (and it turns out the minimum energy configuration is an isoceles triangle with an apex angle of about 80 degree[8]). Note that the presence of atom 3 changes the *pair* interactions – a different V_2 function is required depending on the position of atom 3 ($\mathbf{x_3}$). From elementary chemistry, new linear combinations of the s and p orbitals on all three atoms emerge depending on the positions of all three atoms, so the pair potential picture fails and it is obvious that at least triplet interactions are required $V_3(\mathbf{x_1}, \mathbf{x_2}, \mathbf{x_3})$. This argument can be extended *mutatis mutandis* by adding more and more atoms. In practice for accurate computations, approach fails for practical cluster sizes.

The epiphany needed to break out of this scheme was to admit and treat the origin of the complexity: the electronic structure of the system. The first generation of such methods used single-particle Linear Combination of Atomic Orbitals “tight-binding” recipes for the electronic structure[2] The earliest such calculations used simplified forms for total energies derived from recursion[10] or moment expansions[11, 12] of local electronic densities of states. Soon thereafter, full diagonalization methods were used to compute total energies, for which the electronic component of the total energy came from summing up the electronic eigenvalues of the tight-binding Hamitonian up to the Fermi level, and a balancing repulsive interaction between nuclei was added to obtain a total energy (the potential energy of the configuration). If we think of this “tight-binding total energy functional”, it is clear that it is capable of representing much more complex and spatially non-local behavior than an empirical potential. Sankey and Allen[13] were the first to implement this in 1985, now what we call “tight-binding MD”. So even though the tight-binding Hamiltonians of the time were imperfect, the work was a great advance since many of the “electronic structure” aspects of the computation were correctly handled.

Ab initio of course means “from the beginning”. This is basically ill-defined, since the *beginning* is subjective. Our purist friends down the hall might want us to start with quarks. What it means in practice is a parameter-free approach to computing the electronic ground state energy and associated quantities like forces. Parameter free means no experiments are fit to, and the prescription for the electronic structure and computation of total energy derives from a general theory of an inhomogeneous electron gas as in a solid or molecule (or in principle, but rarely in practice, many-body wavefunctions).

At about the same time as Sankey and Allen, Car and Parrinello[14] did the first calculations adopting the fundamentally appealing approach of using density functional theory to compute total energies and forces. This was the first truly *ab initio* simulation, and the *ab initio* schemes in wide use today are remote descendants of this fundamental work, and where the local orbital methods are concerned also the work of Allen and Sankey. All of these methods assume the Born-Oppenheimer[15] approximation (separating the ionic and electronic degrees of freedom) and the additional approximation of classical mechanics for ionic motion.

---

[2] The tight-binding models themselves were ”empirical”, and required extensive fitting to a variety of experiments that limit their transferability. One should never underestimate the insights possible for thoughtful tight-binding calculations, see the classic work of Harrison[9].

We should also comment that there is a wider world than just MD simulations. Direct MD is sorely limited by the tiny time step (of order 1 fs (10^{-15}s)) to correctly integrate the classical equations of motion. A very important problem is the effective exploration of configuration space for a complex system. Various "energy landscape" methods are now in common use including some with *ab initio* interactions[4].

2.1.5 The difference between *ab initio* and classical MD

Choosing to carry out an *ab initio* simulation requires some understanding of the electronic structure of the system under study. The details of which (of many) *ab initio* codes to employ, technical questions of Brillouin zone integration (to compute total energies, forces, densities of states etc), selection of pseudopotentials[3], basis sets (plane wave cutoffs or local orbitals employed), density functional used, and so on all must be considered. We think that the best attitude here for a beginner facing a specific new problem is to first search the literature for *ab initio* simulations on similar systems, and invoke the same approximations for the new problem. The wonderful database AFLOW "An automatic framework for high-throughput materials discovery" (aflow.org) offers a vast amount of information on structures, band structures, and many other physical quantities as well as high specific information about settings for *ab initio* codes required for a given problem. Frankly, the quickest way to learn *ab initio* methods is probably to begin by collaborating with one of the many groups using these methods.

Conceptually, there is no difference between classical MD with an empirical potential and *ab initio* MD. The distinction is the origin and form of the interatomic potential. For an *ab initio* simulation, the potential and forces derive directly from the electronic structure of the system as the result of a typically computationally demanding computation. Also, "typical" *ab initio* simulations have poor scaling with system size, scaling as at least the cube of the number of atoms. Empirical potentials can usually be formulated to scale linearly with system size, so from a practical point of view one is constrained to moderate-sized systems with *ab initio* calculations. Thus, if one is interested in high precision calculation of local structure, defects etc., it is likely that an *ab initio* method must be used. If instead, one is interested in the low-q tail of the x-ray structure factor (or large distance pair correlations), or say the distribution of nanovoids in a glass, a large model will be required, and empirical potentials will probably be the only game in town.

There are many codes available. Some are free for academic use (such as SIESTA[16], FIREBALL[17], CPMD[18], Quantum Espresso[19] and ABINIT[20]). Others such as VASP require a license. All of these codes are highly impressive resulting from many years of work by excellent researchers and are "mature". SIESTA and FIREBALL both use a local orbital basis set constructed from optimized pseudoatomic orbitals, the other codes use a plane-wave basis set. By no means is this list of codes exhaustive. Local orbital codes offer considerable flexibility with respect to the basis set (ranging from minimal "single-zeta" basis sets to complicated multi-zeta basis with polarization functions etc), and this can be especially helpful for approximate (in the sense of limited basis set) calculations on large systems. Plane wave codes are usually the easiest to use for small systems (up to a few hundred atoms), and come with a well-tested library of pseudopotentials. Highly useful work can be readily carried out on modest worksta-

---

[3] Psuedopotentials are almost universally used to avoid explicitly treating atomic core electrons. For a full discussion, see the treatment by Martin[15]

tions and in some case (notably VASP[21, 22]) GPU acceleration is very helpful. Of course, supercomputers at national centers devote many cycles to *ab initio* MD!

From a practical point of view, no *ab initio* code is entirely a black box. The Achille's heel of *ab initio* simulations is the fact that the Kohn-Sham equations are non-linear. This means, that as self-consistent field (SCF) solution must be found, and this requires some kind of iteration scheme. In certain cases (highly problem and basis set dependent) the iteration may not converge to the solution and may oscillate between two states. In our personal experience, the code VASP does well on SCF iterations and rarely fails to find the solution. If one is interested in metals, far more care is needed with Brillouin zone integrations. Local orbital codes have to be used with care to ensure that the basis set is adequate to represent interatomic interactions, but again, there is a wealth of published work that can help to guide the researcher and the payoff in efficiency relative to a plane wave code may be substantial.

Besides providing the same basic information as a classical MD simulation (say, coordinates as a function of time), there are "fringe benefits": an approximate electronic structure for the model at any time step, local atomic charges, charge densities etc. This allows the researcher to link to the important class of experiments associated with the electronic structure.

2.1.6 Ingredients of DFT

We considered producing a short review of DFT. One of us (DAD) has written at least two such summaries[23, 24]. We will largely eschew this task in this paper, since there are many masterful treatments available. The Nobel lecture of Kohn[25] is easily readable and historically significant. Richard M. Martin[15] has written the gold standard treatment of DFT and *many* important developments that have arisen in the last 20-30 years. The best recent history from another acknowledged master is the recent paper in Reviews of Modern Physics by R. O. Jones[26], who among other things pointed out Dirac's clear and prescient grasp of the concept of DFT prior to 1930.

Still, to make this paper somewhat self contained, we will tersely summarize the basic ideas of DFT and leave the equations to Martin and Jones. Hohenberg and Kohn[27] showed that the electronic density was a suitable function from which to exactly compute the ground state energy $E = E(\rho(\mathbf{r}))$ of *any* inhomogeneous electron gas, that there was a *universal* functional for the energy of the gas, and provided the variational principle to determine $E(\rho)$ on the road toward practical methods. The primacy of this one scalar field $\rho(\mathbf{r})$, rather than an unimaginably complex many-electron wave function[4] was profound both philosophically (eg, to give a better way to "think" about such problems), and also practically, because it led to methods that are readily handled by modern computers. The method was made practical by Kohn and Sham[28], who converted the Hohenberg-Kohn theorem into an effective single-particle problem with a complicated mean or "self-consistent" field in the spirit of the Hartree[29] or Hartree-Fock approximation[30]. The form of the "Kohn-Sham Hamiltonian" is only approximately known, and relies on accurate quantum Monte Carlo calculations on the homogeneous electron gas[31]. The complicated single-particle problem is then solved on some basis set, most commonly plane waves or local orbitals. With the Kohn-Sham eigenvalues and orbitals available, it is easy to compute the single particle density matrix, total energies, forces and indeed many other properties. Such computations typically scale at best with the cube of the number of electrons, so it becomes

---

[4] Kohn argues that it does not make sense to even try to compute many-electron wavefunctions if the number of electrons exceeds about 100 [25].

computationally expensive fast. Attempts to improve the scaling have been somewhat successful, always based ultimately upon the spatial locality of interatomic interactions: at some point, moving a sufficiently remote atom at $\mathbf{R}'$ will make no significant difference on at atom at $\mathbf{R}$ if $|\mathbf{R} - \mathbf{R}'|$ is sufficiently large[32]. As the electronic structure determines the interatomic interactions, it must also determine this range. The quantity providing this information turns out to be the decay of the single-particle density matrix. Depending on the accuracy needed, the range of the density matrix is at least several $\AA$ in semiconductors and farther in metals[33, 34]. A real-space localized representation can be exploited for this purpose too, the "maximally localized" Wannier functions[35], variants of which may be computed efficiently by projection into the occupied electronic subspace[36, 37]. These ranges are fundamental properties of materials and give direct insight into the nonlocality of the interatomic interactions.

2.1.7 What DFT can provide

Standard DFT codes produce a cornucopia of data: total energies, forces, structure, dynamics (these can usually be quite well represented) and atomic charges. The electronic structure is a trickier undertaking if one considers excited states, since DFT is a *ground state* method. To even estimate a hypothetical optical gap, additional methods beyond DFT are required. Of course excited states are required for optical and transport calculations. The band gap problem has been practically addressed by computations with "hybrid functionals", especially the popular Heyd, Scuseria, Enzerhof[38] ("HSE06") approximation. For correlated electrons, computationally demanding methods are possible such as the GW approximation, "dynamical mean field theory" and other topics treated by Martin, Reining and Ceperley[39].

2.1.8 The emerging solution for large systems and long times: Machine Learning

While our palantir is probably murkier than most, we can make one prediction: Machine-Learning (ML) methods will transform this field. The revolution is already underway. Of all the myriad potential uses of ML we are thinking of a specific one: ML based interatomic potentials. There have been several attempts here. We mention the one that we know the most about, the GAP potential[40], owing to our good fortune to collaborate with the pioneers of the method, and direct the reader to the burgeoning literature on the subject.

A naïve but helpful way to think about ML approaches to interatomic potentials is to interpret it as a sophisticated interpolation scheme. An ML potential is of course only as good as the information that is 'fed' to it. The information takes the form of a large number of atomic configurations, and for each of these the total energy and forces on the atoms computed from an accurate (probably DFT) code. The idea is that if enough of these configurations is available, then one could undertake a new simulation only using information in the database – if "new" configurations were close enough to existing conformations in the database to enable sufficiently accurate "interpolation". Of course, the devil is in the details: what does the metric on configuration space "close enough" mean and how does one really "interpolate". After a lot of very ingenious work[41], there are quantitative answers to these questions and furthermore what is not *a priori* obvious is that the method is quite practical.

The GAP potentials are truly of DFT quality, especially for silicon, and *ML has completely leapfrogged DFT in one critical way* – it is rigorously "order-N" – with

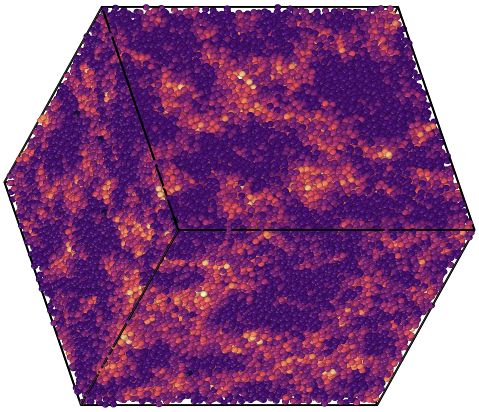

Figure 2.1: Snapshot of a 100,000 atom model of disordered silicon under 12GPa pressure created with OVITO[42], as in Reference[43]. The atoms are color coded according to their coordination: light and dark atoms having high and low coordination respectively, revealing polyamorphism at this pressure.

computational cost scaling linearly with the number of atoms. So ML opens the door to truly enormous simulations and with essentially no loss in accuracy[43]. This linear scaling is a profound feature of the method that guarantees that it will eventually supplant DFT for production runs on large systems. DFT will become the "teacher" of the ML algorithms, and DFT will still have to be used for *terra incognito* – for which no database to learn from exists.

ML can of course provide information beside forces and energies. For example, Cerlotti and co-workers[44] have shown that the electronic density of states can be "learned" and applied this to 100,000-atom simulations of exotic phase changes in disordered phases of silicon under high pressure[43].

We excise an illustration from Ref. [43]: we show a snapshot from a 100,000 atom model of disordered silicon at a pressure of 12 GPa in Fig.2.1. At this particular pressure, polyamorphism is revealed with low and high-density amorphous regions co-existing. The colors indicate coordination (darker, lower coordination). For a full treatment of complex pressure-induced transitions, we refer the reader to the original paper.

2.1.9 A practical aid: Databases

In the United States the so called "Materials Genome Initiative" was introduced more than a decade ago to develop computational methods for materials design to bring advanced technological materials to market sooner. This stimulated efforts in many sectors of academe and produced useful new methods exploiting high performance computing, such as data mining. Impressive databases such as AFLOW now hold

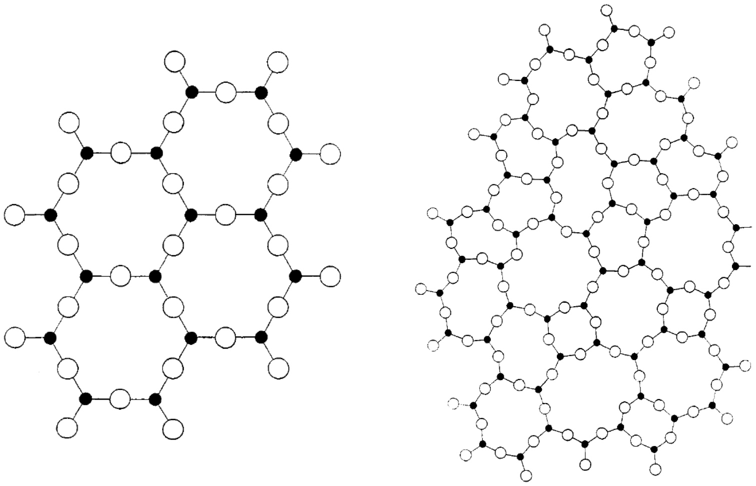

Figure 2.2: **The classic illustration of the continuous random network model:** Two dimensional representation of atomic arrangements in crystalline (left) and glassy A_2O_3.

information on millions of materials, and includes relatively scarce calculations like band structures and thermal properties. It is an ideal site to pick up the threads of an earlier calculation that is a helpful start for something new.

2.2 Methods to produce models

How does one make a computer model of a complex material? In this section, we try to answer these basic questions and explain how the computer simulations are done at present.

In crystals where atoms are arranged periodically, determining the positions of atoms is simple (unless the unit cell itself is complex), and it is easy to imagine filling space with such a unit cell using the lattice vectors. In amorphous systems, devoid of long range order between the atoms, determining the structure can be daunting. The first point to note is that the arrangement of atoms in amorphous systems is *not* random: it lacks long range order but almost always has well defined short range order. The tendency to order decays with distance: second neighbor distances exhibit more variation than the first neighbor, and so on. To illustrate this, the atomic arrangement in a A_2O_3 type glass proposed by Zachariasen [45] has been shown in Fig. 2.2 . Such ordering (or lack therof) on various length scales is well discussed by Elliott[46].

Once a model of an amorphous material is obtained, the first step in the analysis is to compare to experiments. The decay of spatial pair-correlations correlations with distance is a first test that the model must pass since this is an observable inferred from diffraction experiments[4]. The lack of crystal-like long range order obviously makes model generation in amorphous materials challenging but on the brighter side this inherent disorder in atomic positions leads to emergent phenomena unknown in crystals and render amorphous materials to a wide range of applicability. As we stated above, favorable agreement of a model with diffraction data is necessary but is not sufficient. As we discuss below with “Reverse Monte Carlo”, it is relatively easy to make computer models that agree nicely with a structure factor or pair correlation function, but the atomic structure generated from such a fitting has high density of unphysical sturctures eg. chemically unrealistic bond, atypical values of bond lengths, bond angles, etc. This emphasizes the importance of comparing models with experiments measuring diverse physical properties.

The rest of this chapter is organized as follows. First, we discuss the simulation methods used to produce models of amorphous materials, comparing one with other. Second, we discuss how the structural, electronic, and vibrational properties are analyzed from the models. Appropriate comparison with its crystalline counterpart is made whenever possible to create a better understanding of the subject being discussed. We illustrate all this with specific amorphous materials that we hope are both illustrative and interesting in their own right.

2.2.1 Simulation Paradigm: Melt Quench

What we call the “simulation paradigm” is the idea of directly simulating the transition of the material from the liquid phase to an amorphous solid. The melt quench method, as the name suggests, involves creating a high temperature liquid melt of the material and then rapidly quenching it, resulting in a structure with disorder “frozen in” [4]. A starting random configuration of atoms is chosen (with atoms being disallowed to be unphysically close). Periodic boundary conditions are always employed, so that we we are really modeling is a crystal with a large unit cell. This system is heated to a temperature well above its melting point to produce a liquid melt and to make sure that there is diffusive ion dynamics. The melt is cooled to room temperature in subsequent cycles of cooling, using some form of dissipative dynamics, and then equilibration. The structure is ultimately subjected to a force minimization to reduce forces to near zero. The hope is that the final model consistent with experimental observables.

There are many details to be selected for the melt quenching, especially the choice of cooling rate. There is no real *a priori* theory for selecting these rates and the usual way to proceed is to try several cooling rates and verify that the results are acceptably converged (eg the topology does not change significantly with slower quenches). The cooling rates used in simulations are always drastically faster than the physical cooling rates, and it is interesting that melt quench simulations work well for many materials, despite this difference. For a highly detailed study of the effect of cooling rates on structure, see the ML simulations of Bernstein *et al.* for amorphous silicon [47].

As an example, a melt quench simulation of *Cu*- doped Ta_2O_5 [48], made with a cooling rate of 100 K/ps, is presented here. This material is a promising candidate for Conducting Bridge Random Access Memory (CBRAM) memory devices. The *Cu* atoms tend to cluster, and their connectivity can be modified electrochemically creating insulating and conducting phases. Models produced with melt quenching at different cooling rates were able to capture the process of the segregation of the *Cu* atoms from the forming tantala network as the melt was cooled. The presence of the inter connected *Cu* atoms in the network is evident in the *Cu-Cu* correlation in Fig. 2.3.

The melt-quench method always begs difficult questions. (1) Is the model big enough? (2) Are there artifacts from the use of periodic boundary conditions (PBC)? (3) Are the cooling rates used in the simulation acceptably “slow”? (4) Is it sufficient to compute energies and forces using only the Γ point of the Brillouin zone associated with the periodic boundary conditions?

Firstly, the term “big enough” can be subjective and the size of the model that can

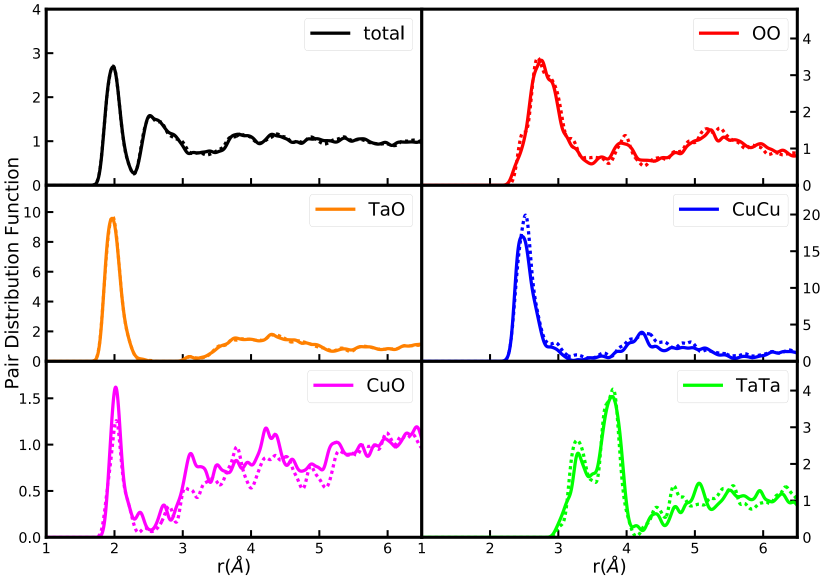

Figure 2.3: Pair distribution function for Model I (**solid line**) and Model II (**dotted line**) of amorphous Cu-doped tantala [48] with same number of atoms and differing only in their cooling rates.

be generated depends significantly on the nature of the interatomic interactions used during the melt-quench process. For example, performing DFT based calculation on VASP limits the system size to a few hundreds atoms. On the other hand, calculation with empirical potentials can have millions of atoms in the system. As usual there is an intelligent balancing required between size, time scales and accuracy. The choices depend also on the questions the researcher is attempting to answer.

The use of PBC allows us to perform MD of the bulk material by removing surface effects and rendering the system as a crystal with a large unit cell. One should be careful with the system size when using the PBC: the size of the supercell must be greater than the cut-off distance of the interatomic potential to avoid self interaction among atoms and their images in other cells. The PBC allows meaningful information on a length-scale half the size of the simulation box [23]. There are analogous artifacts for computations of lattice vibrations[23]. Also size and PBC artifacts are strongly **k** and **r** dependent in S(**k**) and g(**r**) respectively. To check if the system is free of artifacts from PBC, one should perform the simulations with different sized simulation box and compare the results.

Cooling rate is a critical parameter that determines the credibility of the generated amorphous models. Overly short cooling rates can produces several artifacts, like remnants of the liquid melt, because the system will not have enough time to thoroughly explore the configuration space. Typical cooling rates used for MQ methods using VASP is of the order of 100-200 K/ps. Also note that classical molecular dynamics code could use a much slower cooling rate but is still far from comparable to the actual process in lab.

Calculations of energy and forces requires summation over the Brillouin zone and the accuracy depends solely on the way the zone is sampled. However, for amorphous systems that lack translational are usually represented by large supercells containing hundreds of atoms. Such large supercells have a commensurately small Brillouin zone [49] and thus the calculation using a single k-point (Γ-point) may be acceptable in amorphous systems. This point is explored in detail in Ref. [50].

2.2.2 Information Paradigm

The idea of this method is to produce models that agree with experimental information. It differs from the melt quench method as the idea is to construct models directly using implied experimental information instead of trying to simulate the glass formation process. The idea was first adopted by Kaplow and co-workers [51] to make vitreous Se models consistent with X-ray radial distribution function. The idea was later developed by McGreevy and Puzstai [52] who named it Reverse Monte Carlo (RMC). A more recent idea is the empirical potential structure relaxation (EPSR) by Soper that starts with an empirical potential which is modified recursively by the difference between the model and the experimental data [53].

This idea of this "inverse modeling" scheme is to find a set of atomic coordinates that minimizes the discrepancy between the model and the experiment. The quantity measuring this discrepancy, for a set of atomic coordinates $\vec{R}$, is defined as:

$$\chi^2(\mathbf{R}) = \sum_i \frac{[F_E(Q_i) - F_m(\mathbf{R}, Q_i)]^2}{\sigma_i^2} \tag{2.1}$$

where $F_E(Q_i)$ is the experimental value of the quantity at point Q_i and $F_m(\vec{R}, Q_i)$ is the value calculated from the model. σ_i is a non-negative quantity associated with the experimental error. In simple words, χ^2 measures the goodness of fit and the inverse modeling is merely a problem of finding a set of atomic coordinates that render a minimum χ^2 (eg small enough to fit within experimental error bars). Note that in practice there are a vast number of such minima, and it begs the question: "which minimum do we accept"? One can get out of a trapped configuration with a Monte Carlo minimization [54] accepting an atomic move that increases χ^2 with a positive non-zero probability.

An attractive feature of this method is that it does not require interatomic potentials for the minimization and thus presents particular promise in systems where the energy calculations are prohibitively expensive. The approach honors experimental data by construction, the weakness however is that none of these algorithms took a course in freshman chemistry – so a model of amorphous SiO_2 made in this way would have many O-O and Si-Si bonds, which are essentially physically nonexistent[5].

2.2.3 Teaching chemistry to RMC: FEAR

How do we include all the information available during the process of model construction, viz. experimental information and accurate interatomic interactions? This might be achieved through unification of simulation and information paradigm thereby changing the problem to the minimization of the quantity

$$\phi = E(\mathbf{R}) + \chi^2 \Lambda \tag{2.2}$$

---

[5] *Ad hoc* constraints can be included, introducing a "penalty" for homopolar bonds, for example. This is somewhat unsatisfying however, since it introduces bias from the modeler.

where $\Lambda(> 0)$ determines the relative weighting of the experiment and potential [55]. We do not follow this program because determining Λ is ambiguous and we find better results with alternative techniques. The first alternative, called Experimentally Constrained Molecular Relaxation (ECMR) [56], employs a self-consistent iteration scheme that involved completely converged RMC minimization and energy minimization. Often, the configuration gets trapped in a local minimum and requires a new start.

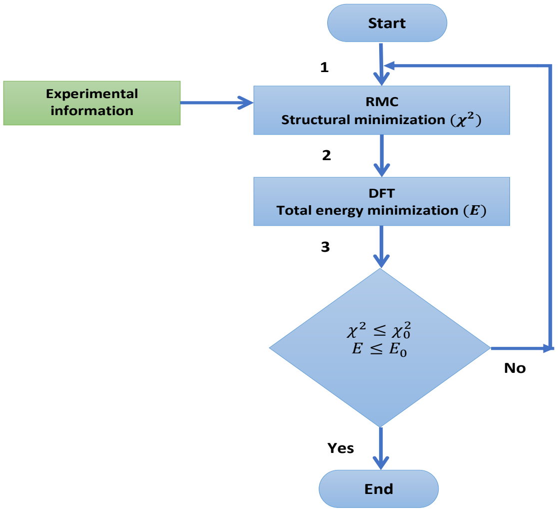

Figure 2.4: Flowchart of FEAR method.

A successful technique for minimizing ϕ in equation (2.2) is called *Force Enhanced Atomic Refinement* (FEAR) [57, 58, 59]. In contrast to the completely converged minimization in ECMR, FEAR involves separate incremental minimization of the quantities thus reducing the chances of getting stuck in a local minima. The fact that the models generated agree reasonably well with experiment and also sit in an energy minimum of a suitable interatomic interactions greatly increases the credibility of the models. FEAR modeling shows particular promise in reducing the computational effort needed to produce models compared to the melt quench process.

A schematic diagram of the FEAR technique has been given in Fig. 2.4. It has been applied to a wide range of amorphous materials ranging from *a*-Si [57] and *a*-C [60] to bulk metallic glasses [61] and sodium-silicates[62]. Recently FEAR has been employed in a high precision study of annealing induced changes in the intermediate range ordering of zirconia-doped tantala, a possible candidate for LIGO mirror coatings [63].

It is reasonable to describe FEAR as a way to "invert" the scattering data to obtain a realistic computer model. Of course this is true only in a statistical sense – there is of course no hope of *uniquely* inverting pair correlations into coordinates in space, but with the inclusion of chemical information incorporated through the partial energy minimizations, a highly representative result reflective both of the experiment and chemistry can be obtained.

A representative example of FEAR modeling in $Pd_{40}Ni_{40}P_{20}$ bulk metallic glass is presented here. Two models were generated for this work, one with 200 atoms using melt quench technique and the other with 300 atoms using FEAR. Fig.2.5 suggests that the models generated have successfully reproduced the structural features implied by the experiment as confirmed by the agreement of the radial distribution function of the models with the experiment. Since this multi-component system has several (unknown) partial pair-correlation functions (thereby making the total correlation less informative than for elemental system), we also compute Extended X-ray Fine Absorption Structure (EXAFS) to gain valuable first shell information. The experimental data [65] is shown by red dots connecting line, FEAR and MQ models are represented by the blue and black lines respectively. The inset in each figure shows the EXAFS spectrum, i.e. $\left(k^2\chi(k)\right)$. The FEAR300 model shows a better agreement with the experimental EXAFS spectra. The corresponding Fourier transformations of FEAR300 and MQ200 is plotted alongside experimental values [65] and it is observed FEAR300 model is qualitatively in better agreement with the experiment.

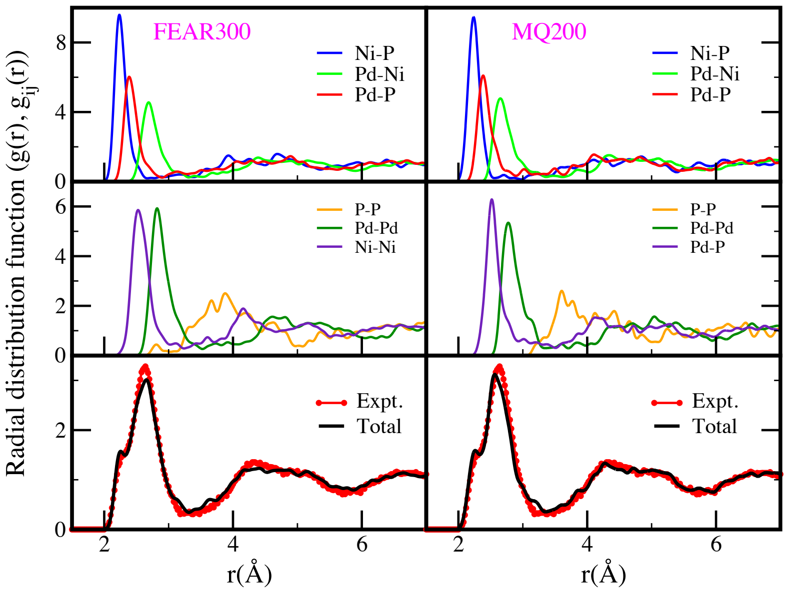

Figure 2.5: We show comparison of our $Pd_{40}Ni_{40}P_{20}$ models, made with melt-quench (MQ200) and FEAR (FEAR300) [61] method, with the experiment [64]. The radial distribution function $(g(r))$ is in good agreement with the experiment and the partial RDF are also consistent with previous literature.

The FEAR model, despite being 100 atoms larger than the melt quench, used only 16% of the total computer time used by the melt quench model. This computational efficiency could be utilized to produce larger computer models of materials with a identical computational resource.

2.2.4 Gap Sculpting

A common drawback of the melt-quench MD simulation is that it produces structural models with greater disorder than the real material. The excess disorder can range from

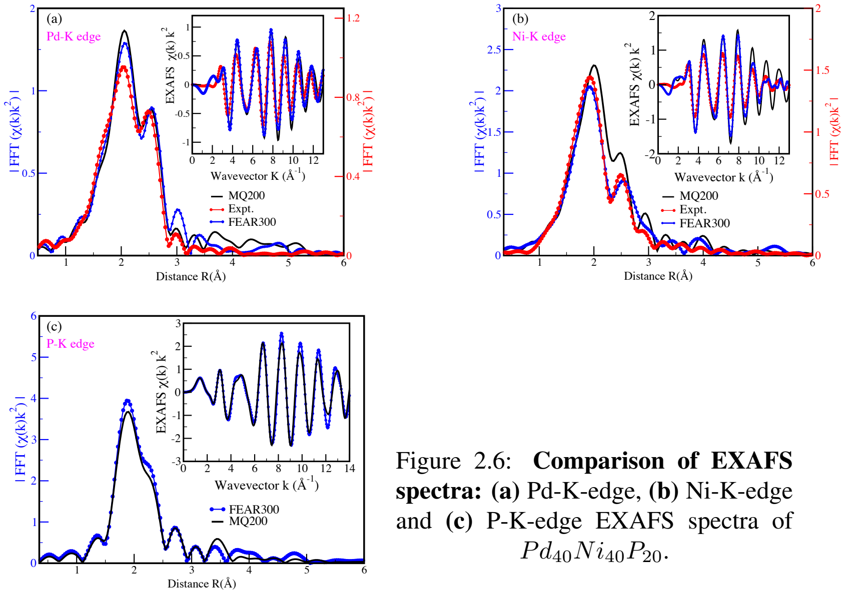

Figure 2.6: **Comparison of EXAFS spectra: (a)** Pd-K-edge, **(b)** Ni-K-edge and **(c)** P-K-edge EXAFS spectra of $Pd_{40}Ni_{40}P_{20}$.

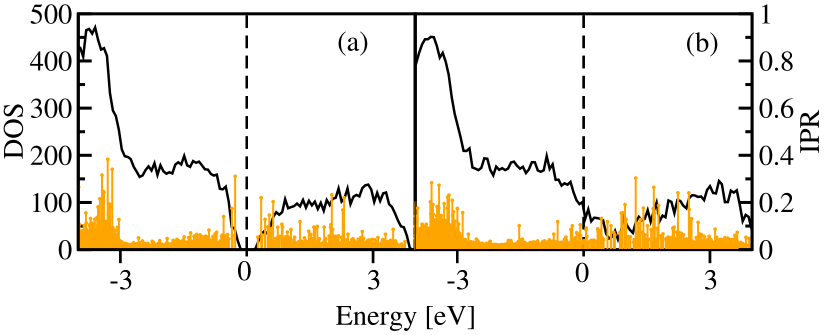

Figure 2.7: The (black curve) electronic density of states (DOS) and (orange drop lines) Inverse Participation Ratio (IPR) of the insulating model (a) and the metallized model (b). The energy axis for all data sets is shifted to have Fermi level at 0 eV (highlighted by the broken vertical line).

acute short-range defects like coordination defects to more subtle defects in medium range like presence of irregular sized rings. While the extent of the discrepancy depends on the systems as well as modeling approach, the issue is universal. Often one possesses experimental information about optical gaps and defects. It may also be desirable to explore the possibility of obtaining a desired band gap. To enable this, we discuss “Gap Sculpting”.

Many approaches have been proposed to remedy the above drawback – most focus either on better potential/pseudopotential or on better sampling of the potential energy landscape. Gap sculpting, proposed in 2016 and applicable to all electronic strucuture based MD simulation takes a completely different approach.

To understand the method of gap sculpting, it is necessary to start by appreciating the universal correlation between structural defects and electronic defects. It is a common knowledge that the short-range structural defects like dangling and floating bonds, anomalous bond angles etc often give rise to defect states in the electronic band gap. The Urbach tails, observed as the exponential tapering of band edges on various crystalline and amorphous materials, are attributed to disorders in the network, eg. long and short bond lengths[66], disorder at the medium range [67]. It has been shown by many researchers that atomic models with improved structural orders are also the ones with few electronic defects[68]. Gap sculpting is based on the converse of this observation – a model with fewer electronic defects should also be the one with fewer structural defects. In that regard, gap sculpting modifies the atomic forces in MD simulation so that the electronic defects in the band gap are explicitly disfavored. In practice, this takes the form of a biased dynamics where the total forces on atoms are given by [69, 70]

$$\mathbf{F}_{\alpha}^{BS} = -\sum_{i}^{occ} \langle \Psi_i\,(r)\,|\frac{\partial H}{\partial R_{\alpha}}|\Psi_i\,(r)\rangle = -\sum_{i}^{occ} \frac{\partial \lambda_i}{\partial R_{\alpha}}. \tag{2.3}$$

Here, λ_i is the eigenvalue of the Hamiltonian *H* corresponding to *i*th eigenstate Ψ_i, and R_α are the *3N* positional degrees of freedom. The gradient $\frac{\partial \lambda_i}{\partial R_\alpha}$ provides the direction in configuration space for maximum increase of λ_i - so gives information about how to move atoms to maximally affect λ_i. Eigenstates with eigenvalues in an *a priori* known energy range can be forced out of that range using a biasing force given by [70]:

$$\mathbf{F}_{\alpha}^{bias} = -\sum_{i:E_{min}<\lambda_i<E_{max}} \gamma g(\lambda_i)\langle \Psi_i\,(r)\,|\frac{\partial H}{\partial R_{\alpha}}|\Psi_i\,(r)\rangle. \tag{2.4}$$

This biasing force pushes the states below and above the Fermi level in opposite directions. The quantity γ is merely a knob to control the magnitude of the biasing forces. The method also is ideal and frankly easier to use to study metallization-closing gap rather than opening. In this case one shepherds electronic level toward the Fermi level. It is important to note here that the biasing forces derived from the standard Hellmannn-Feynmann forces which are already computed in any electronic-structure-based MD simulation and thus the method adds negligible computational overhead compared to the standard MD simulation.

As an example of the application of the metallization technique, we present an insulator to metal transition achieved in amorphous $(GeSe_3)_{1-x}Ag_x$ [71] glasses using suitable biasing forces. The melt-quench models made using VASP [72] with PBE [73] exchange-correlation functional and had 240 atoms with *x* = 0.15 and 0.25. Conducting structures were obtained by annealing the starting configuration using biased forces at 700 K for 18 ps. The electronic states in the energy range [ϵ_F-0.4eV,ϵ_F+0.4eV] were included in the computation of the biasing forces and a γ = 3.0 was used. The biasing potential moves the electronic states at the band edges into the band-gap region. This causes the force biased structure to have states in the band gap (obtained with MD without biasing forces) thereby inducing metallic characters. After obtaining the "biased models" we relaxed and annealed the models with "unbiased" forces. The density of states (DoS) and the inverse participation ratio (measuring the localization of the states) are compared between the model with no biased forces (insulating model) and the model with biased forces (metallized model) are shown in Fig.2.7. The presence of extended states in the metallized models clearly suggests conducting behavior. The final metallic models were found to be almost energetically identical to the insulating phase, an interesting "electronic polyamorphism".

2.3 Analyzing the models

Once a model is created it is subject to different analysis depending upon researchers' interest. The analysis performed test the validity and credibility of the model by allowing comparison with the experiment. The results obtained from the analysis often guide future theoretical as well as experimental studies.

2.3.1 Structure

Structural analysis of the models is the first pivotal test amid the lack of a well defined positions of the atoms like in crystals. Since amorphous materials inherently lack long range order, characteristic of crystalline materials, the order usually extends up to the second nearest set of neighbors, sometimes called the medium range order. The first test is to check whether or not the arrangement of atoms represent an amorphous systems. Other test include, but are not limited to, bonding environment calculation, coordination number, Voronoi polyhedra analysis, and voids.

2.3.1.1 Radial Distribution function

The radial distribution function (RDF) is defined as:

$$g(r) = \frac{N}{V}\frac{dn(r)}{4\pi r^2 dr} \tag{2.5}$$

where N and V denote the total number of atoms and the volume of the simulation box respectively. dn(*r*) denotes the number of atoms located at distances lying between *r* and *r* +d*r*[74]. The radial distribution function g(*r*) gives the probability of finding an atom in a shell of thickness d*r* at a distance *r* from a reference atom. For systems having more than one atom type, the partial radial distribution function is defined as:

$$g_{\alpha\beta}(r) = \frac{N}{V}\frac{dn_{\alpha\beta}(r)}{4\pi r^2 dr}c_\alpha \tag{2.6}$$

where c_α is the concentration of α atomic species. The functions $g_{\alpha\beta}(r)$ denotes the normalized probability of finding an atom of type β at a distance *r* from the reference α atom.

The qualitative information portrayed by the RDF can be easily understood from Fig. 2.8 comparing the RDF in amorphous and crystalline form of Carbon at nearly same density. In crystalline materials, if one leaves out positional uncertainty arising from thermal vibrations, which is not a crude approximation at room temperature, then the probability of finding an atom at certain distance from another is precisely known because of the inherent long range order/periodicity. This certainty is marked by sharp peaks in the RDF at specific distances and vanishing elsewhere as seen in Fig. 2.8. However, when a system is amorphous, the sharp peaks are flattened and there is in fact no order after 4.0 $\AA$ in amorphous Carbon as seen in Fig. 2.8. A basic point from Fig. 2.8 is the identical location of the first peak in both amorphous and crystalline Carbon suggesting the presence of a well-defined short range order, though with modest bond-length and bond-angle distortions [75], in amorphous material and thereby invalidating preconception of a random distribution of atoms in amorphous materials that a first time reader may have in mind.

It is a common practice in the amorphous research community to take the position of the minimum after the first peak as defining coordination in amorphous systems and

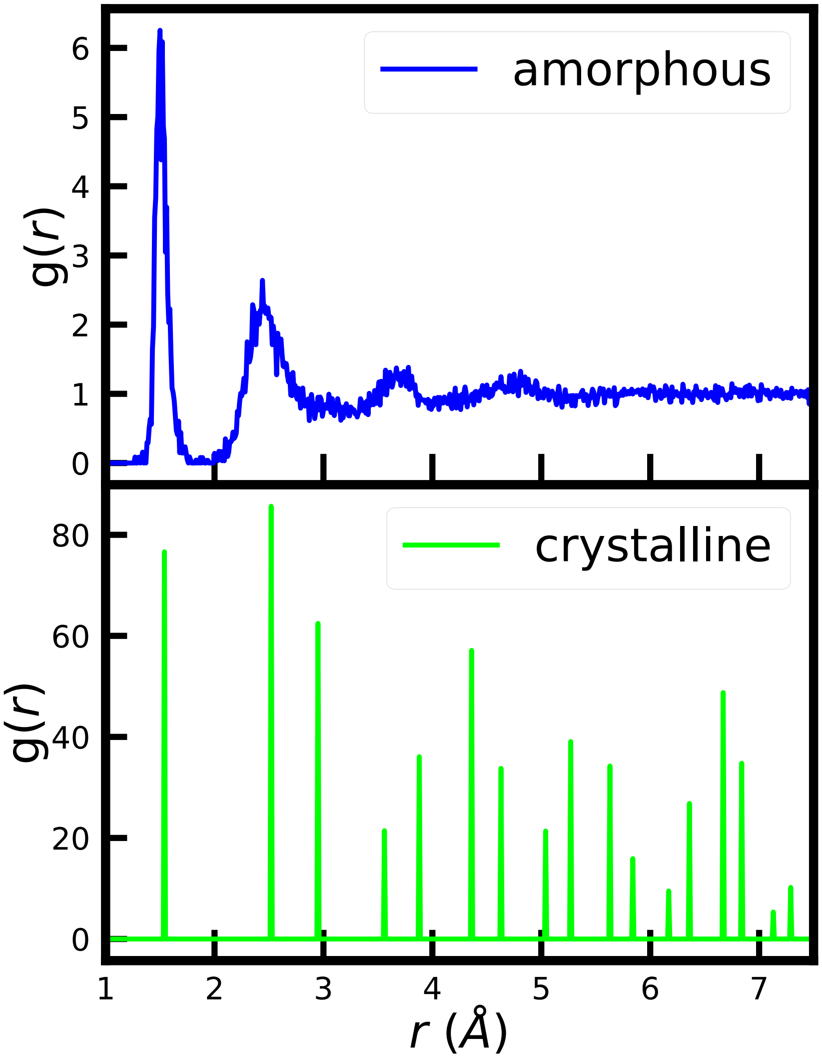

Figure 2.8: Comparison of RDF of crystalline (diamond) and amorphous Carbon [60] at 3.50 gm/cc.

the area under the first peak gives an estimate of the coordination number of an atom in the sample. The second peak gives information on a longer length scale: in transition metal oxides like a-Ta_2O_5, the first peak gives idea of the metal-oxygen bonds while the second peak provides information about the connection among the metal-oxygen polyhedra [63].

A lot of different definitions of the same or similar symbols and their additive and/or multiplicative constants within the correlation functions often cause confusion. To clear any confusion with the definitions and to compare several different definitions used by different research groups, we suggest the reader to go through the work of David Keen comparing these functions [76]. Also for readers interested in the reciprocal space counterpart of the RDF, the structure factor S(Q), we suggest going through Ref.[76, 74, 52].

2.3.1.2 Voronoi Analysis

Computer models represent a set of particles (atoms, molecules) in space and hence their properties are governed by the ordering of such particles. Providing a compact but full characterization of the structure of materials is still a challenge. Voronoi analysis is a step forward in that direction. It determines the local structure of a particle considering the arrangement of the neighbors around that central particle [77]. For a fixed set of particles, a Voronoi cell of the central particle is the region in space closer to that particle than any other. This 3D geometry is characterized by a set of indices, called Voronoi indices, written in the form $\langle\ n_3\ n_4\ n_5\ n_6\ \rangle$ where n_i denotes the number of faces with *i* edges present in the Voronoi cell. A perfect icoshedra has $\langle$ 0 0 12 0 $\rangle$ Voronoi indices. The analysis of Voronoi indices often provide useful information on the Voronoi cell dynamics which can be used to study glass forming ability and glass transition in glasses.

Voronoi analysis is applicable to a wide range of materials ranging from defected crystals and deformed polycrystals to glasses and liquids [77]. It can be used to study how the crystalline structure is compromised at higher temperatures [77]. In a bulk metallic glass ($Cu_{46}Zr_{46}Al_8$), a class of amorphous materials, it has been used to study the evolution of certain Voronoi indices near the glass transition temperature which have slow dynamics believed to be responsible for the excellent glass forming ability of the material [78].

2.3.2 Electronic Structure

Amorphous materials have widespread electronic applications ranging from solar cells to light sensors and optical memory devices to conducting bridge random access memory (CBRAM). Electronic structure not only serves to validate (or invalidate) the model but also can be used as *a priori* information to produce materials with desired electronic properties [71, 70, 69] as discussed in Section 2.2.4. The change in electronic structure with doping is important, as it renders materials with potentially important applications.

2.3.2.1 Electronic Density of States

The lack of periodicity and long range order in amorphous materials rules out the possibility of describing electrons as Bloch states as in crystals. However, the density of states (DoS) is a equally valid description of the electron states in both crystals and amorphous materials and is defined as:

$$g\left(E\right)=\frac{1}{V}\sum_{n}\delta\left(E-E_n\right) \tag{2.7}$$

where *g(E)* is the DoS per unit volume per unit energy interval and V is the volume of the system [79]. The electronic DoS in amorphous materials is qualitatively similar to that of its crystal counterpart except that that sharp edges expected in crystals are smoothed out due to disorder into “band tails” [75, 66].

In analogy to crystals, amorphous materials can be classified as insulators, semiconductors, and conductors based on the nature of the DoS and the spatial extent of

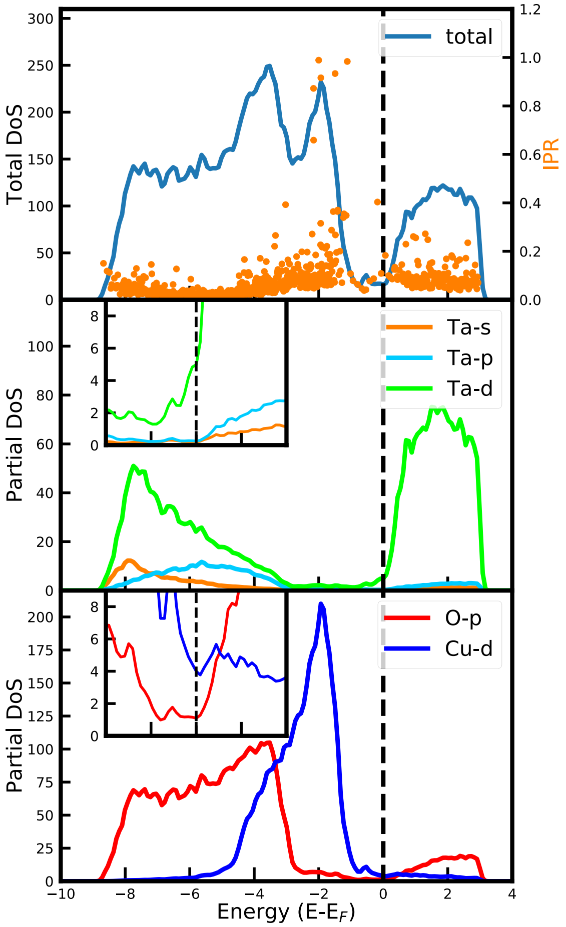

Figure 2.9: Electronic DoS and inverse participation ratio (IPR) of *Cu*- doped Ta_2O_5 indicating conducting behavior due to the states created in the gap by the added *Cu* atoms[48].

the wavefunctions. Amorphous semiconductors like a-Si possess conduction and valence band and a clear band gap whereas, for bulk metallic glass like $Pd_{40}Ni_{40}P_{20}$ [61], which is conducting, there is no band gap. Doping can sometimes transform an insulating host conducting by creating states in the band gap of the insulating host. For example, *Cu*-doping in Ta_2O_5 to be conducting by generating states in the band gap arising mostly from the *Cu*-atoms as shown in Fig.2.9. The partial density of states show contribution of individual atomic species to the total DoS. It is only the states near the Fermi level that play a significant role in determining conduction mechanisms.

Apart from the information about whether the material is conducting or not, DoS also gives valuable information about the presence of defects and impurities. For example, the localized states in the band gap of a-Si is a consequence of the intrinsic three-fold and five-fold defects, often known as dangling and floating bonds, present in the model [80, 68].

Electronic band gap evaluated with LDA, GGA and PBE functionals never agree closely to the experimental value since DFT is a ground state theory. One can overcome this shortcoming by using hybrid functional like Hyed-Scuseria-Ernzerhof (HSE06) [81, 82] that produce band gaps close to the experimental values [83].

2.3.2.2 Inverse Participation Ratio

Another quantity of importance is the inverse participation ratio (IPR)[84] which indicates whether the electron states are extended (distributed throughout the sample) or concentrated/localized at some atoms. Due to the inherent disorder present in amorphous materials, electronic states can be localized in certain region or a certain site. If one has the contributions to the electronic states (or eigenvectors) from different atomic orbitals the IPR for a state (ψ_n) can be calculated as:

$$\mathcal{I}(\psi_n) = \frac{\sum_{orb} |a_n^{orb}|^4}{\left(\sum_{orb} |a_n^{orb}|^2\right)^2} \tag{2.8}$$

where a_n^{orb} is the contribution to ψ_n from a particular local orbital and the sum runs over the atomic orbitals of all the atoms present. The mathematical form implies that localized states have high IPR value. For example, if ψ_n has a contribution arising only from a particular orbital of a particular atom, the IPR would be unity. On the other hand, a completely extended state produces a value of (1/*N*), i.e. evenly distributed over *N* atoms. Localized states (near the Fermi level) have a zero d.c. conductivity while extended states have a finite conductivity at O K. In other words, the only way for conduction between localized states is by means of thermally assisted "hopping" [79]. IPR is important but qualitative and depends for example on the basis set employed. An example of extended states in *Cu*- doped tantala [48] is shown in Fig. 2.9.

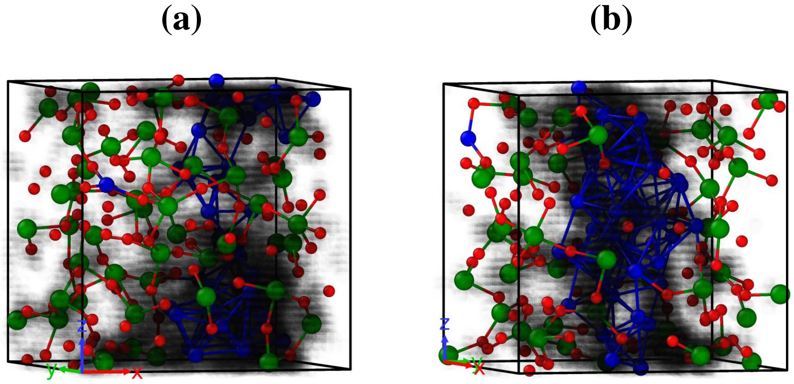

Figure 2.10: Space Projected Conductivity scalar field for Model I(**a**) and Model II(**b**) of Cu-doped tantala models [48] shown in grayscale. Those parts of the network containing the interlinked *Cu*-atoms are clearly more conducting in both models. The electrical conductivity of Model II is about 5 times that of Model I, because of the more robust *Cu* filament of Model II.

2.3.2.3 Space Projected Conductivity

Conduction in amorphous materials depends mainly on two quantities: the density of states providing information about the species contributing near the Fermi-level and the localization of the electronic states and momentum matrix elements between Kohn-Sham states near the Fermi level. Recently, a spatial decomposition of the Kubo-Greenwood [85, 86] developed by our group provides information about conducting paths in real space by projecting the conductivity onto real space grids. By introducing a discrete grid in space, we show that the quantity:

$$\zeta(\mathbf{x}) = \left| \sum_{\mathbf{x}'} \Gamma(\mathbf{x}, \mathbf{x}') \right| \tag{2.9}$$

provides such information at the spatial grid point **x** and for which:

$$\Gamma(\mathbf{x}, \mathbf{x}') = \sum_{ij\alpha} g_{ij} \xi^{\alpha}_{ij}(\mathbf{x}) (\xi^{\alpha}_{ij}(\mathbf{x}'))^{*}. \tag{2.10}$$

Here, g_{ij} is defined in *Prasai et. al* [87] and $\xi^{\alpha}_{ij}(\mathbf{x}) \equiv \psi^{*}_{i}(\mathbf{x}) p^{\alpha} \psi_{j}(\mathbf{x})$ is a complex-valued function, $\psi_i(\mathbf{x})$ is the i^{th} Kohn-Sham eigenfunction and $p^{\alpha} = \frac{\hbar}{i} \frac{\partial}{\partial x_{\alpha}}, (\alpha = x, y, z)$. We have used this approach to describe transport in a solid electrolyte material[87], *Cu* -doped *a-alumina*[88], and most recently on other materials [89]. For a more detailed discussion on SPC we suggest the reader to go through Ref.[89].

As an example of this technique, we have shown the SPC calculations of Cu-doped tantala models discussed in Section 2.2.1 in Fig.2.10. The grayscale shows that interconnected Cu-atoms are form the most active conduction part in the otherwise insulating tantala host.

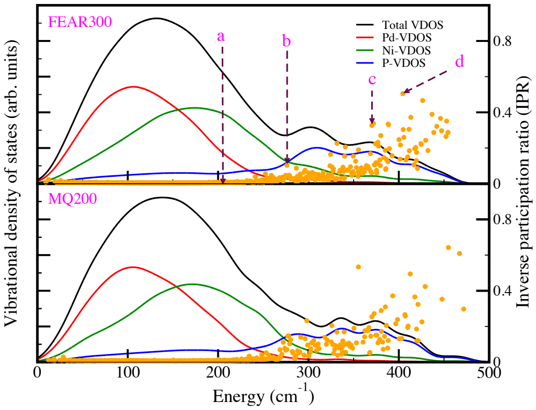

Figure 2.11: Vibrational DoS and VIPR of two different models of $Pd_{40}Ni_{40}P_{20}$ bulk metallic glass[61].

2.3.3 Vibrational Properties

Vibrations of atoms in solids, both crystalline and amorphous, form an important part of analysis because it is directly related to transport and thermal properties. The vibrational behavior of amorphous solids are similar to their crystalline counterpart except for the fact that the lack of periodicity smears out the sharp features (Van-Hove singularities) in amorphous materials [90].

Vibrational density of states (VDoS) is an observable that can be measured experimentally most directly using inelastic neutron scattering. Most often, the vibrational properties are calculated using the harmonic approximation and small finite displacements[90]. VDoS can also be calculated from the velocity auto correlation function that uses the trajectory given by a thermal MD simulation[23]. Details of the theory behind calculation of the normal modes can be found elsewhere [91, 90]. Standard MD codes such as VASP and LAMMPS[92] offer such computations. The quantity of importance is the VDoS defined as:

$$g(\omega) = \frac{1}{3N} \sum_{i=1}^{3N} \delta\left(\omega - \omega_i\right) \tag{2.11}$$

where N is the number of atoms and ω_i is the 3N eigenfrequencies. Thus, evaluating the VDoS reduces to a problem finding the ω_i's for the system. The calculation of these eigenfrequencies are a routine task in most simulation packages including VASP [72][6]. In physical terms, the quantity $g(\omega)d\omega$ represents the number of modes within the interval $[\omega, \omega + d\omega]$. The delta function on the right hand side of Eqn. 2.11 is approximated by a Gaussian with a suitable standard deviation [7].

In multi-atomic systems, the contribution to the VDoS from each atomic species, called partial VDoS, can be calculated as:

$$g_\alpha(\omega) = \frac{1}{3N} \sum_{i=1}^{N_\alpha} \sum_{n} \left|e_i^n\right|^2 \delta\left(\omega - \omega_n\right) \tag{2.12}$$

where, e_i^n are the eigenvectors of the normal modes, N_α is the number of atom of species α. The partial VDoS must satisfy $g\left(\omega\right) = \sum_\alpha g_\alpha(\omega)$, a relation that can be used to check if the partial VDoS is correctly calculated. The general trend in the partial VDoS is that lighter atoms contribute towards higher frequency vibrations while heavier atoms contribute towards lower frequency vibrations.

Presence of disorder in the arrangement of atoms in amorphous materials can often lead to localization of vibrational modes with some analogy to electron states. While the VDoS is an experimental observable, the localization of the vibrational modes are not easily observable in experiments. The extent of localization of vibrational modes in computer models can be measured with a quantity called vibrational inverse participation ratio (VIPR) defined as:

$$\nu\left(\omega_n\right) = \frac{\sum_{i=1}^{N} \left|\mathbf{u}_n^i\right|^4}{\left(\sum_{i=1}^{N} \left|\mathbf{u}_n^i\right|^2\right)^2} \tag{2.13}$$

where $\left(\mathbf{u}_n^i\right)$ is the displacement vector of the i^{th} atom in the normal mode frequency ω_n. By definition, if a particular normal mode is completely localized on a single

---

[6] Note for VASP users: Relax the model with zero pressure relaxation before the vibration calculations. Often times, problems arise when there are more than three imaginary eigenfrequecies in VASP output after the vibrational calculation. To get rid of this problem, I recommend relaxing the system to a better energy and force convergence (lower EDIFF and EDIFFG) and re-running the vibrational calculation.

[7] $\sigma \approx 1 - 2\%$ of the maximum eigenfrequency

atom, the VIPR would be unity, while on the other hand a vibrational modes that are extended over large number of atoms have smaller VIPR value. Often times in literature researchers use the term participation ratio defined as the inverse of VIPR.

A representative example for the VDoS and VIPR for a bulk metallic glass $(Pd_{40}Ni_{40}P_{20})$ has been shown in Fig.2.11. The figure shows localization of high frequency normal modes that are localized on the lightest atoms,i.e. P- atoms.

2.4 Conclusion

We have outlined some of the aspects of *ab initio* simulations of disordered systems. We explained the similarities and differences of *ab initio* and classical methods. We intentionally avoided the mathematical intricacy of a first principles approach as this is well treated elsewhere. We described methods for creating computer models of materials and emphasized the differences between direct "melt quench" and information based approaches. We discussed FEAR in some detail. We also pointed out the possibility of exploring models with desired optical/electronic properties in the Gap Sculpting section. We then discussed some common methods for characterizing models and/or comparing to experiments including structural, electronic and vibrational signatures of models. In the spirit of analyzing models, in systems for which electrical conductivity is relevant, we described a recently developed method to project conductivity onto real space grids to determine those parts of a material that may provide conduction.

2.5 Acknowledgements

We thank the National Science Foundation (NSF) for support under DMR award 1507670. We also acknowledge Extreme Science and Engineering Discovery Environment (XSEDE), supported by NSF grant number ACI-1548562, for providing computational resources under DMR-190008P. We offer special thanks to Dr. Kiran Prasai for his help with the manuscript. We would also like to thank Dr. Volker Deringer for providing us the figure for the disordered silicon under pressure, Fig. 2.1.

Bibliography

[1] W.H. Bragg and W.L. Bragg. The reflection of x-rays by crystals. *Proceedings of the Physical Society. A*, 88:428–438, 1913.

[2] Alexander Wlodawer, Wladek Minor, Zbigniew Dauter, and Mariusz Jaskolski. Protein crystallography for aspiring crystallographers or how to avoid pitfalls and traps in macromolecular structure determination. *The FEBS Journal*, 280(22):5705–5736, 2013.

[3] Ruth Rowlands, Anita Zeidler, Henry E Fischer, and Philip S Salmon. Structure of the intermediate phase glasses gese3 and gese4: The deployment of neutron diffraction with isotope substitution. *Frontiers in Materials*, 6, jun 2019.

[4] D. A. Drabold. Topics in the theory of amorphous materials. *The European Physical Journal B*, 68(1), 2009.

[5] Erik Holmberg. On the Clustering Tendencies among the Nebulae. II. a Study of Encounters Between Laboratory Models of Stellar Systems by a New Integration Procedure. *apj*, 94:385, nov 1941. Provided by the SAO/NASA Astrophysics Data System.

[6] A. Rahman. Correlations in the motion of atoms in liquid argon. *Phys. Rev.*, 136:A405–A411, Oct 1964.

[7] M.P Allen and D.J. Tildesley. Oxford University Press, second edition, 2017.

[8] Otto Sankey, David Niklewski, D. Drabold, and John Dow. Molecular-dynamics determination of electronic and vibrational spectra, and equilibrium structures of small si clusters. *Physical review. B, Condensed matter*, 41:12750–12759, 07 1990.

[9] Walter A Harrison. *Electronic structure and the properties of solids : the physics of the chemical bond*. Freeman, San Francisco, Calif., 1980.

[10] W. Matthew C. Foulkes and Roger Haydock. Tight-binding models and density-functional theory. *Phys. Rev. B*, 39:12520–12536, Jun 1989.

[11] A P Sutton, M W Finnis, D G Pettifor, and Y Ohta. The tight-binding bond model. *Journal of Physics C: Solid State Physics*, 21(1):35–66, jan 1988.

[12] A.E. Carlsson. Beyond pair potentials in elemental transition metals and semiconductors. volume 43 of *Solid State Physics*, pages 1 – 91. Academic Press, 1990.

[13] Otto F. Sankey and Roland E. Allen. Atomic forces from electronic energies via the hellmann-feynman theorem, with application to semiconductor (110) surface relaxation. *Phys. Rev. B*, 33:7164–7171, May 1986.

[14] R. Car and M. Parrinello. Unified approach for molecular dynamics and density-functional theory. *Phys. Rev. Lett.*, 55:2471–2474, Nov 1985.

[15] Richard M. Martin. *Electronic Structure: Basic Theory and Practical Methods*. Cambridge University Press, second edition, 2020.

[16] Jose M Soler, Emilio Artacho, Julian D Gale, Alberto Garcia, Javier Junquera, Pablo Ordejon, and Daniel Sanchez-Portal. The siesta method for ab initio order-n materials simulation. *Journal of Physics: Condensed Matter*, 14(11):2745–2779, mar 2002.

[17] James P. Lewis, Pavel Jelínek, José Ortega, Alexander A. Demkov, Daniel G. Trabada, Barry Haycock, Hao Wang, Gary Adams, John K. Tomfohr, Enrique Abad, Hong Wang, and David A. Drabold. Advances and applications in the fireball ab initio tight-binding molecular-dynamics formalism. *physica status solidi (b)*, 248(9):1989–2007, 2011.

[18] R. Car and M. Parrinello. Unified approach for molecular dynamics and density-functional theory. *Phys. Rev. Lett.*, 55:2471–2474, Nov 1985.

[19] Paolo Giannozzi, Stefano Baroni, Nicola Bonini, Matteo Calandra, Roberto Car, Carlo Cavazzoni, Davide Ceresoli, Guido L Chiarotti, Matteo Cococcioni, Ismaila Dabo, Andrea Dal Corso, Stefano de Gironcoli, Stefano Fabris, Guido Fratesi, Ralph Gebauer, Uwe Gerstmann, Christos Gougoussis, Anton Kokalj, Michele Lazzeri, Layla Martin-Samos, Nicola Marzari, Francesco Mauri, Riccardo Mazzarello, Stefano Paolini, Alfredo Pasquarello, Lorenzo Paulatto, Carlo Sbraccia, Sandro Scandolo, Gabriele Sclauzero, Ari P Seitsonen, Alexander Smogunov, Paolo Umari, and Renata M Wentzcovitch. Quantum espresso: a modular and open-source software project for quantum simulations of materials. *Journal of Physics: Condensed Matter*, 21(39):395502 (19pp), 2009.

[20] X. Gonze, B. Amadon, P.-M Anglade, Jean-Michel Beuken, François Bottin, P. Boulanger, F. Bruneval, D. Caliste, Razvan Caracas, Michel Côté, Thierry Deutsch, Luigi Genovese, Philippe Ghosez, M. Giantomassi, S. Goedecker, D. Hamann, Patrick Hermet, F. Jollet, Gérald Jomard, and J. Zwanziger. Abinit: First-principles approach to material and nanosystem properties. *Computer Physics Communications*, 180:2582–2615, 12 2009.

[21] Mohamed Hacene, Ani Anciaux-Sedrakian, Xavier Rozanska, Diego Klahr, Thomas Guignon, and Paul Fleurat-Lessard. Accelerating vasp electronic structure calculations using graphic processing units. *Journal of Computational Chemistry*, 33(32):2581–2589, 2012.

[22] M. Hutchinson and M. Widom. Vasp on a gpu: Application to exact-exchange calculations of the stability of elemental boron. *Computer Physics Communications*, 183(7):1422 – 1426, 2012.

[23] D.A. Drabold. Molecular dynamics simulation of network glasses. In P Boolchand, editor, *Insulating and Semiconducting Glasses*, pages 607–652. World Scientific, Singapore, 2000.

[24] D.A. Drabold. Recent developments in modeling of amorphous materials. In M. Mitkova, M.N. Kozicki, G. Lucovsky, and M. Popescu, editors, *Non-crystalline materials for optoelectronics*. INOE, Burachest, 2004.

[25] W. Kohn. Nobel lecture: Electronic structure of matter—wave functions and density functionals. *Rev. Mod. Phys.*, 71:1253–1266, Oct 1999.

[26] R. O. Jones. Density functional theory: Its origins, rise to prominence, and future. *Rev. Mod. Phys.*, 87:897–923, Aug 2015.

[27] P. Hohenberg and W. Kohn. Inhomogeneous electron gas. *Phys. Rev.*, 136:B864–B871, Nov 1964.

[28] W. Kohn and L. J. Sham. Self-consistent equations including exchange and correlation effects. *Phys. Rev.*, 140:A1133–A1138, Nov 1965.

[29] D.R. Hartree. The Wave Mechanics of an Atom with a Non-Coulomb Central Field. Part I. Theory and Methods. *Proceedings of the Cambridge Philosophical Society*, 24(1):89, Jan 1928. Provided by the SAO/NASA Astrophysics Data System.

[30] V. Fock. Approximation method for the solution of quantum mechanical multi-body problems. *Zeitschrift fur Physik*, 61(1-2):126–148, jan 1930.

[31] D. M. Ceperley and B. J. Alder. Ground state of the electron gas by a stochastic method. *Phys. Rev. Lett.*, 45:566–569, Aug 1980.

[32] E. Prodan and W. Kohn. Nearsightedness of electronic matter. *Proceedings of the National Academy of Sciences*, 102(33):11635–11638, 2005.

[33] Kiran Prasai, Parthapratim Biswas, and D A Drabold. Electrons and phonons in amorphous semiconductors. *Semiconductor Science and Technology*, 31(7):073002, jun 2016.

[34] Xiaodong Zhang and D. A. Drabold. Properties of the density matrix from realistic calculations. *Phys. Rev. B*, 63:233109, May 2001.

[35] Nicola Marzari and David Vanderbilt. Maximally localized generalized wannier functions for composite energy bands. *Phys. Rev. B*, 56:12847–12865, Nov 1997.

[36] Uwe Stephan and David A. Drabold. Order-n projection method for first-principles computations of electronic quantities and wannier functions. *Phys. Rev. B*, 57:6391–6407, Mar 1998.

[37] Uwe Stephan, Richard M. Martin, and David A. Drabold. Extended-range computation of wannier-like functions in amorphous semiconductors. *Phys. Rev. B*, 62:6885–6888, Sep 2000.

[38] Aliaksandr V. Krukau, Oleg A. Vydrov, Artur F. Izmaylov, and Gustavo E. Scuseria. Influence of the exchange screening parameter on the performance of screened hybrid functionals. *The Journal of Chemical Physics*, 125(22):224106, 2006.

[39] Richard M. Martin, Lucia Reining, and David M. Ceperley. *Interacting Electrons: Theory and Computational Approaches*. Cambridge University Press, 2016.

[40] Volker L. Deringer, Miguel A. Caro, and Gábor Csányi. Machine learning interatomic potentials as emerging tools for materials science. *Advanced Materials*, 31(46):1902765, 2019.

[41] Keith T. Butler, Daniel W. Davies, Hugh Cartwright, Olexandr Isayev, and Aron Walsh. Machine learning for molecular and materials science. *Nature*, 559(7715):547–555, jul 2018.

[42] Alexander Stukowski. Visualization and analysis of atomistic simulation data with OVITO–the open visualization tool. *Modelling and Simulation in Materials Science and Engineering*, 18(1):015012, dec 2009.

[43] V.L. Deringer, N. Bernstein, G. Csányi, C. Ben Mahmoud, M. Ceriotti, M. Wilson, D.A. Drabold, and S. R. Elliott. Origins of structural and electronic transitions in disordered silicon. *Nature*, 589, 2021.

[44] Chiheb Ben Mahmoud, Andrea Anelli, Gábor Csányi, and Michele Ceriotti. Learning the electronic density of states in condensed matter. *Phys. Rev. B*, 102:235130, Dec 2020.

[45] W. H. Zachariasen. The atomic arrangement in glass. *Journal of the American Chemical Society*, 54:3841–3851, Oct 1932.

[46] S. R. Elliott. Strucutre. In *Physics of amorphous materials*, pages 53–134. Longman Scientific and Technical, New York, 1984.

[47] Noam Bernstein, Bishal Bhattarai, Gábor Csányi, David A. Drabold, Stephen R. Elliott, and Volker L. Deringer. Quantifying chemical structure and machine-learned atomic energies in amorphous and liquid silicon. *Angewandte Chemie International Edition*, 58(21):7057–7061, 2019.

[48] Rajendra Thapa, Bishal Bhattarai, M. N. Kozicki, Kashi N. Subedi, and D. A. Drabold. Structure and charge transport of amorphous cu doped ta2o5: An ab initio study. *Phys. Rev. Materials*, 4:064603, Jun 2020.

[49] Peter Kratzer and Jörg Neugebauer. The basics of electronic structure theory for periodic systems. *Frontiers in Chemistry*, 7:106, 2019.

[50] D. A. Drabold, J. D. Dow, P. A. Fedders, A. E. Carlsson, and Otto F. Sankey. Convergence of force calculations for noncrystalline si. *Phys. Rev. B*, 42:5345–5348, Sep 1990.

[51] Roy Kaplow, T. A. Rowe, and B. L. Averbach. Atomic arrangement in vitreous selenium. *Phys. Rev.*, 168:1068–1079, Apr 1968.

[52] R. L. McGreevy and L. Pusztai. Reverse monte carlo simulation: A new technique for the determination of disordered structures. *Molecular Simulation*, 1(6):359–367, 1988.

[53] A. K. Soper. Partial structure factors from disordered materials diffraction data: An approach using empirical potential structure refinement. *Phys. Rev. B*, 72:104204, Sep 2005.

[54] Nicholas Metropolis, Arianna W. Rosenbluth, Marshall N. Rosenbluth, Augusta H. Teller, and Edward Teller. Equation of state calculations by fast computing machines. *The Journal of Chemical Physics*, 21(6):1087–1092, 1953.

[55] Michael Habeck, Wolfgang Rieping, and Michael Nilges. Weighting of experimental evidence in macromolecular structure determination. *Proceedings of the National Academy of Sciences*, 103(6):1756–1761, 2006.

[56] Parthapratim Biswas, De Tafen, and D. Drabold. Experimentally constrained molecular relaxation: The case of glassy $GeSe_2$. *Phys. Rev. B*, 71, 02 2005.

[57] A. Pandey, P. Biswas, and D. A. Drabold. Inversion of diffraction data for amorphous materials. *Scientific Reports*, 6:33731, 2016.

[58] A. Pandey, P. Biswas, and D. A. Drabold. Force-enhanced atomic refinement: Structural modeling with interatomic forces in a reverse mont carlo approach applied to amorphous Si and SiO_2. *Phys.Rev.B*, 92:155205, 2015.

[59] A. Pandey, P. Biswas, B. Bhattarai, and D. A. Drabold. Realistic inversion of diffraction data for an amorphous solid: The case of amorphous silicon. *Phys.Rev.B*, 94:235208, 2016.

[60] Bishal Bhattarai, Anup Pandey, and D.A. Drabold. Evolution of amorphous carbon across densities: An inferential study. *Carbon*, 131:168 – 174, 2018.

[61] Bishal Bhattarai, Rajendra Thapa, and D A Drabold. Ab initio inversion of structure and the lattice dynamics of a metallic glass: the case ofpd40ni40p20. *Modelling and Simulation in Materials Science and Engineering*, 27(7):075002, jul 2019.

[62] Qi Zhou, Tao Du, Lijie Guo, Morten Mattrup Smedskjær, and Mathieu Bauchy. New insights into the structure of sodium silicate glasses by force-enhanced atomic refinement. *Journal of Non-Crystalline Solids*, 536, may 2020.

[63] K. Prasai, J. Jiang, A. Mishkin, B. Shyam, S. Angelova, R. Birney, D. A. Drabold, M. Fazio, E. K. Gustafson, G. Harry, S. Hoback, J. Hough, C. Lévesque, I. MacLaren, A. Markosyan, I. W. Martin, C. S. Menoni, P. G. Murray, S. Penn, S. Reid, R. Robie, S. Rowan, F. Schiettekatte, R. Shink, A. Turner, G. Vajente, H-P. Cheng, M. M. Fejer, A. Mehta, and R. Bassiri. High precision detection of change in intermediate range order of amorphous zirconia-doped tantala thin films due to annealing. *Phys. Rev. Lett.*, 123:045501, Jul 2019.

[64] Stephan O. Hruszkewycz. *The effect of fluctuation microscopy constraints on reverse Monte Carlo models of metallic glass structure*. PhD thesis, 2009.

[65] Vijay Kumar, T. Fujita, K. Konno, M. Matsuura, M. W. Chen, A. Inoue, and Y. Kawazoe. Atomic and electronic structure of $Pd_{40}Ni_{40}P_{20}$ bulk metallic glass from ab initio simulations. *Phys. Rev. B*, 84:134204, Oct 2011.

[66] Y. Pan, F. Inam, M. Zhang, and D. A. Drabold. Atomistic origin of urbach tails in amorphous silicon. *Phys. Rev. Lett.*, 100:206403, May 2008.

[67] A. Amato, S. Terreni, M. Granata, C. Michel, B. Sassolas, L. Pinnard, M. Canepa, and G. Cagnoli. Observation of a correlation between internal friction and urbach energy in amorphous oxides thin films. *Scientific Reports*, 10, Feb 2020.

[68] Dale Igram, Bishal Bhattarai, Parthapratim Biswas, and D.A. Drabold. Large and realistic models of amorphous silicon. *Journal of Non-Crystalline Solids*, 492:27 – 32, 2018.

[69] Kiran Prasai, Parthapratim Biswas, and D. Drabold. Sculpting the band gap: A computational approach. *Scientific Reports*, 5, 06 2015.

[70] Kiran Prasai, Parthapratim Biswas, and David Alan Drabold. Electronically designed amorphous carbon and silicon. *physica status solidi (a)*, 213(7):1653–1660, 2016.

[71] Kiran Prasai, Gang Chen, and D. Drabold. Amorphous to amorphous insulator-metal transition in $\mathrm{GeSe_3}$:Ag glasses. *Physical Review Materials*, 1, 03 2017.

[72] G. Kresse and J. Furthmuller. Efficient iterative schemes for ab initio total-energy calculations using a plane-wave basis set. *Phys. Rev. B*, 54:11169–11186, Oct 1996.

[73] John P. Perdew, Kieron Burke, and Matthias Ernzerhof. Generalized gradient approximation made simple. *Phys. Rev. Lett.*, 77:3865–3868, Oct 1996.

[74] Sébastien Le Roux and Valeri Petkov. *ISAACS* – interactive structure analysis of amorphous and crystalline systems. *Journal of Applied Crystallography*, 43(1):181–185, Feb 2010.

[75] D.A. Drabold and T. Abtew. Defects in amorphous semiconductors: Amorphous silicon. In D.A. Drabold and S.K. Estreicher, editors, *Theory of Defect in Semiconductors*, Topics in Applied Physics, pages 245–268. Springer Berlin Heidelberg, New York.

[76] David A. Keen. A comparison of various commonly used correlation functions for describing total scattering. *Journal of Applied Crystallography*, 34(2):172–177, Apr 2001.

[77] Emanuel A. Lazar, Jian Han, and David J. Srolovitz. Topological framework for local structure analysis in condensed matter. *Proceedings of the National Academy of Sciences*, 112(43):E5769–E5776, 2015.

[78] Rajendra Thapa, Kashi Nath Subedi, Bishal Bhattarai, and David A. Drabold. Forced enhanced atomic refinement modeling of the metallic glass cu46zr46al8. *physica status solidi (b)*, n/a(n/a):2000415.

[79] S. R. Elliott. Electrons. In S. R. Elliott, editor, *Physics of amorphous materials*, pages 173–246. Longman Scientific and Technical, New York, 1984.

[80] Sokrates T. Pantelides. Gap states in amorphous silicon—dangling and floating bonds. *Journal of Non-Crystalline Solids*, 97-98:79 – 82, 1987. Amorphous and liquid semiconductors.

[81] Jochen Heyd, Gustavo E. Scuseria, and Matthias Ernzerhof. Erratum: "hybrid functionals based on a screened coulomb potential" [j. chem. phys. 118, 8207 (2003)]. *The Journal of Chemical Physics*, 124(21):219906, 2006.

[82] Aliaksandr V. Krukau, Oleg A. Vydrov, Artur F. Izmaylov, and Gustavo E. Scuseria. Influence of the exchange screening parameter on the performance of screened hybrid functionals. *The Journal of Chemical Physics*, 125(22):224106, 2006.

[83] Raghuveer Chimata. Optical properties of materials calculated from first principles theory, 2010.

[84] J. M. Ziman. *Models of disorder*. Cambridge University Press, 1979.

[85] R. Kubo. Statistical mechanical theory of irreversible processes. I. General theory and simple applications to magnetic and conduction problems. *J. Phys. Soc. Jpn.*, 12:570–586, 1957.

[86] D. A. Greenwood. The Boltzmann equation in the theosry of electrical conduction in metals. *Proceedings of the Physical Society*, 71:585–596, 1958.

[87] Kiran Prasai, Kashi N. Subedi, Kaelyn Ferris, Parthapratim Biswas, and David A. Drabold. Spatial projection of electronic conductivity: The example of conducting bridge memory materials. *physica status solidi (RRL) – Rapid Research Letters*, 12(9):1800238, 2018.

[88] K. N. Subedi, K. Prasai, M. N. Kozicki, and D. A. Drabold. Structural origins of electronic conduction in amorphous copper-doped alumina. *Phys. Rev. Materials*, 3:065605, Jun 2019.

[89] Kashi N. Subedi, Kiran Prasai, and David A. Drabold. Space-projected conductivity and spectral properties of the conduction matrix. *physica status solidi (b)*, page 2000438.

[90] S. R. Elliott. Vibrations. In *Physics of amorphous materials*, pages 135,172. Longman Scientific and Technical, New York, 1984.

[91] Bishal Bhattarai and D.A. Drabold. Vibrations in amorphous silica. *Journal of Non-Crystalline Solids*, 439:6 – 14, 2016.

[92] Steve Plimpton. Fast parallel algorithms for short-range molecular dynamics. *Journal of Computational Physics*, 117(1):1 – 19, 1995. lammps.sandia.gov.